Nanoscale Tubules Formed by Exfoliation of Potassium Hexaniobate

Geoffrey B. Saupe, Chad C. Waraksa, Hyuk-Nyun Kim, Yong J. Han, David M. Kaschak, Diana M. Skinner, and Thomas E. Mallouk*

Department of Chemistry, The Pennsylvania State University, University Park, Pennsylvania 16802

Received December 21, 1998. Revised Manuscript Received March 27, 2000

The exfoliation of acid-exchanged $K_4Nb_6O_{17}$ with tetra(*n*-butyl)ammonium hydroxide in water produces a colloidal suspension of individual sheets, which roll into loosely bound tubular structures. The tubule shape can be made permanent via precipitation of the colloid with alkali cations. Atomic force microscopy and transmission electron micrographs reveal that the tubules have outer diameters ranging from 15 to 30 nm and that they are 0.1 to 1 μm in length. The observed curling tendency, preferential folding, and cleavage angles of the individual sheets are interpreted in terms of the crystal structure of the parent solid, $K_4Nb_6O_{17}$. The driving force for tubule formation appears to be relief of strain that is inherent in the asymmetric single sheets. This driving force is absent in bilayer colloids formed early in the exfoliation process, which are found only as flat sheets. Tubules in colloidal suspensions that have been subjected to turbulence have a tendency to unroll into flat sheets on surfaces, indicating that the forces controlling rolling and unrolling are closely balanced.

Introduction

One of the important goals of materials chemistry is to develop ways of tailoring the structure of matter on the nanometer length scale. Structurally well-defined building blocks are potentially useful in the synthesis of designed catalysts, photonic band gap materials, nanoscale electronic devices, and chemical separations media.[1] The growing "toolbox" for making these composite materials contains both organic and inorganic components, which come in a variety of shapes and dimensionalities, including spherical and polyhedral clusters, rigid rods, and sheets. Tubular structures are particularly interesting in this regard, because of their inherent mechanical strength,[2] their unusual electronic transport properties,[3] and their ability to act as containers or capsules.[4] Consequently, the synthesis and characterization of organic[5] and carbon- and boronitride-based nanotubes[6] have recently been subjects of intense research activity.

While tubular structures are ubiquitous in living systems and are increasingly common in supramolecular organic chemistry,[7] they are actually quite rare among inorganic compounds. Fibrous minerals such as chrysotile consist of sheets that curl into nanoscale rolls, to relieve built-in strain between silicate and brucite layers.[8] Synthetic inorganic tubules have been made from lamellar solids such as MoS_2 and WS_2, in a manner analogous to forming multiwall nanotubes from a material (carbon) that is thermodynamically more stable as a lamellar solid.[9] There are also various templating methods that have been used to prepare metal, metal oxide, and metal sulfide tubes[10−12] and hollow fiber sol−gel materials such as silica.[13]

In the course of studying the chemical transformation of lamellar oxides into single-sheet colloids, we observed that one of these compounds, $K_{4-x}H_xNb_6O_{17}$ ($x \approx 3$), produces a colloid with unusual properties. The X-ray

(1) (a) Ozin, G. A. *Adv. Mater.* **1992**, *4*, 612. (b) Mann, S. J. *Chem. Mater.* **1997**, *9*, 2300. (c) Ying, J. Y. WTEC Workshop Rep. *R&D Status Trends Nanoparticles, Nanostructured Materials, Nanodevices, U.S. Proc.* (1998), Meeting Date 1997; International Technology Research Institute: Baltimore, MD, 1998; pp 96−99. (d) Yaghi, O. M.; Li, H.; Davis, C.; Richardson, D.; Groy, T. *Acc. Chem. Res.* **1998**, *31*, 474.

(2) Ajayan, P. M.; Stephan, O.; Colliex, C.; Trauth, D. *Science* **1994**, *265*, 1212.

(3) Tans, S. J.; Devoret, M. H.; Dai, H.; Thess, A.; Smalley, R. E.; Geerligs, L. J.; Dekker, C. *Nature* **1997**, *386*, 474.

(4) (a) Valdes, C.; Spitz, Urs P.; Toledo, L.; Leticia, M.; Kubik, S. W.; Rebek, J., Jr. *J. Am. Chem. Soc.* **1995**, *117*, 7, 12733. (b) Allcock, H. R. *Acc. Chem. Res.* **1976**, *9*, 5120.

(5) (a) Schnur, J. M. *Science.* **1993**, *262*, 1669. (b) Ghadiri, M. R.; Granja, J. R.; Milligan, R. A.; McRee, D. E.; Khazanovich, N. *Nature* **1993**, *336*, 324. (c) Gattuso, G.; Menzer, S.; Nepogodiev, S. A.; Stoddart, J. F.; Williams, D. J. *Angew. Chem., Int. Ed. Engl.* **1997**, *36*, 1451. (d) Yager, P.; Schoen, C. D.; Price, R.; Singh, A. *Biophys. J.* **1985**, *48*, 899. (e) Kogiso, M.; Hanada, T.; Yase, K.; Shimizu, T. *Chem. Commun.* **1998**, 1791.

(6) (a) Iijima, S. *Nature* **1991**, *354*, 56. (b) Stephan, O.; Ajayan, P. M.; Colliex, C.; Redlich, Ph.; Lambert, J. M.; Bernier, P.; Lefin, P. *Science* **1994**, *266*, 1683. (c) de Heer, W. A.; Chatelain, A.; Ugarte, D. *Science* **1995**, *268*, 845. (d) Chopra, N. G.; Luyken, R. J.; Cherrey, K.; Crespi, V. H.; Cohen, M. L.; Louie, S. G.; Zettl, A. *Science* **1995**, *269*, 966. (e) Li, W. Z.; Xie, S. S.; Qian, L. X.; Chang, B. H.; Zou, B. S.; Zhou, W. Y.; Zhao, R. A.; Wang, G. *Science* **1996**, *274*, 1701. (f) Saito, S. *Science* **1997**, *278*, 77. (g) Ebbesen, T. W. *J. Phys. Chem. Solids* **1997**, *58*, 1979. (h) Yakobson, B. I.; Smalley, R. E. *Am. Sci.* **1997**, *85*, 324. (i) Rao, C. N. R.; Sen, R.; Satishkumar, B. C.; Govindaraj, A. *J. Chem. Soc., Chem. Commun.* **1998**, 1525. (j) Ebbesen, T. W. *Acc. Chem. Res.* **1998**, *31*, 558.

(7) König, B. *Angew. Chem., Int. Ed. Engl.* **1997**, *36*, 1833.

(8) Frazier, S. E.; Bedford, J. A.; Hower, J.; Kenney, M. E. *Inorg. Chem.* **1967**, *6*, 1693.

(9) (a) Tenne, R.; Margulis, L.; Genut, M.; Hodes, G. *Nature* **1992**, *360*, 444. (b) Feldman, Y.; Wasserman, E.; Srolovits, D. J.; Tenne, R. *Science* **1995**, *267*, 222. (c) Feldman, Y.; Frey, G. L.; Homyonfer, M.; Lyakhovitskaya, V.; Margulis, L.; Cohen, H.; Hodes, G.; Hutchison, J. L.; Tenne, R. *J. Am. Chem. Soc.* **1996**, *118*, 5362.

(10) Lakshmi, B. B.; Patrissi, C. J.; Martin, C. R. *Chem. Mater.* **1997**, *9*, 2544.

(11) Hoyer, P. *Langmuir* **1996**, *12*, 1411.

(12) Zelenski, C. M.; Dorhout, P. K. *J. Am. Chem. Soc.* **1998**, *120*, 734.

(13) Ono, Y.; Nakashima, K.; Sano, M.; Kanekiyo, Y.; Inoue, K.; Hojo, J.; Shinkai, S. *J. Chem. Soc., Chem. Commun.* **1998**, 1477.

10.1021/cm981136n CCC: $19.00
Published on Web 05/11/2000

diffraction patterns of the restacked colloids did not show the series of layer lines that were characteristic of chemically similar materials, such as $KTiNbO_5$, KNb_3O_8, and $KCa_2Nb_3O_{10}$.[14] Also, the rheological and mechanical properties of concentrated colloids were suggestive of a fibrous material, rather than a lamellar one. In this paper, we report a microscopic examination of these colloids, which shows that they consist of both sheets and high aspect ratio tubules. The latter are predominant in concentrated colloidal suspensions. The procedure used to prepare these tubules is essentially the same as that reported in two recent publications by Domen et al.,[15] although the formation of tubular structures was not considered in those papers. We show here that their results can be reinterpreted by considering that the colloidal particles are predominantly tubules, rather than multilamellar strips as proposed.

$K_4Nb_6O_{17}$ is a structurally and chemically well characterized material. Its synthesis, crystal structure, and dielectric properties were reported almost 30 years ago.[16] Since then, several investigations have elucidated its intercalation chemistry,[17] the structural details of its hydration,[18] and its photoluminescence behavior.[19] Domen and co-workers have extensively investigated $K_4Nb_6O_{17}$ as a photocatalyst. They have shown that $K_4Nb_6O_{17}$ is a wide band gap semiconductor, which acts as an effective catalyst for the photolysis of water and alcohols under UV light when modified with interlayer Ni or Pt clusters.[20] Recently, they have also prepared ion-exchangeable, spin-coated films of $K_4Nb_6O_{17}$.[21] Related studies in our laboratory have focused on the layer-by-layer assembly of thin films of this material[22] and have exploited the properties of surface-modified, platinized $K_4Nb_6O_{17}$ in the photolysis of HI with visible light.[23]

In most of this prior work, it has been noted that the individual niobium oxide sheets are polar and that this unusual structural feature gives rise to two different interlamellar environments for intercalation. In bulk crystals of $K_4Nb_6O_{17}$ and its intercalation compounds, the face-to-face juxtaposition of sheets constrains them to be planar. We show here that once exfoliated, the asymmetric sheets spontaneously curl into tubules. The driving force for tubule formation appears to be essentially the same as in crysotile, i.e., inherent mechanical strain in the unilamellar sheets, which causes curling along certain specific crystal directions.

Experimental Section

Synthesis of $K_4Nb_6O_{17}$ and $KTiNbO_5$. Reagent-grade K_2CO_3, TiO_2, and Nb_2O_5 (99.99%) were obtained from Aldrich and used as received. $K_4Nb_6O_{17}$ and $KTiNbO_5$ were prepared by heating finely ground mixtures of the appropriate metal oxides and K_2CO_3 in alumina crucibles (Coors). The temperature was held at 900 °C for 1 h before continuing to heat at 1050 °C for 24 h. K_2CO_3 was used in slight excess (10 mol %) to replace any material volatilized during heating. The phase purity of these compounds was confirmed by X-ray powder diffraction.[24]

Elemental Analysis. C, H, N, and Cl analyses were done by Atlantic Microlabs, Norcross, GA. K was determined by flame atomic absorption spectroscopy (FAAS), using a potassium cathode lamp. Samples were prepared by dissolving the solid in a minimum amount of 48% HF and then diluting with water.

Nitrogen adsorption measurements were performed at 77 K using a Micromeritics ASAP 2000 surface area analyzer. The adsorption data were fit to pore size distributions using a density functional theory (DFT) algorithm developed for microporous materials.[25] X-ray diffraction measurements were made with a Phillips X'Pert MPD diffractometer, using monochromatized Cu Kα radiation. Computer-assisted graphic molecular modeling was done with CAChe software.

Acid Exchange and Exfoliation of $K_4Nb_6O_{17}$. A total of 1.75 g $K_4Nb_6O_{17}$ was stirred in 300 mL of a 1−3 M HCl solution for 1 week at 40 °C to produce $K_{4-x}H_xNb_6O_{17}$. The solid was separated by filtration and rinsed with distilled water, and the acid solution was renewed four times to promote complete exchange. The final product was rinsed with water, and then dried in air at 20 °C. The degree of exchange for this sample was $x = 3.2 \pm 0.1$, as determined by FAAS. Next, an aqueous solution of tetra(*n*-butyl)ammonium hydroxide (TBA^+OH^-, 40 wt %, Aldrich) was added dropwise to ∼0.5 g of the acid-exchanged solid in 50 mL of water while stirring, until the solution pH stabilized around 10. In the colloid used in the acid−base titration, the starting pH was about 12 (4.55 mol TBA^+OH^- per mol $K_{0.8}H_{3.2}Nb_6O_{17}$) and the entire suspension was titrated. For the colloids used in the rest of the experiments, the exfoliated solutions were allowed to stand still for 1−2 h and the top 75% of the solution in the flask (∼70% of the solids) was removed and used for the experiments. The concentration of the colloids was determined by precipitating 5 mL of the suspension with HCl, centrifuging and rinsing with water 3 times, drying in air at 20 °C, and weighing. Typically, the colloidal suspensions used contained 9−10 mg solids/mL.

Precipitation of the Colloid. A total of 0.179 g of KCl or NaCl was dissolved in 20 mL of water and was quickly poured into 30 mL (10 mg/mL) of the colloid. This mixture was allowed to stand for 2 h and was rinsed with copious amounts of water. The (K^+ or Na^+):$[Nb_6O_{17}]^{4-}$ mole ratio was 8:1, i.e., in sub-

(14) Fang, M.; Kim, C. H.; Mallouk, T. E. *Chem. Mater.* **1999**, *11*, 1519.

(15) Abe, R.; Shinohara, K.; Tanaka, A.; Hara, M.; Kondo, J.; Domen, K. *J. Mater. Res.* **1998**, *13*, 861. (b) Abe, R.; Shinohara, K.; Tanaka, A.; Hara, M.; Kondo, J.; Domen, K. *Chem. Mater.* **1997**, *9*, 2179.

(16) Nassau, K.; Shiever, J. W.; Bernstein, J. L. *J. Electrochem. Soc.* **1969**, *116*, 348.

(17) (a) Lagaly, G.; Beneke, K. *J. Inorg. Nucl. Chem.* **1976**, *38* (8), 1513. (b) Kinomura, N.; Kumada, N.; Muto, F. *J. Chem. Soc., Dalton Trans.* **1985**, *11*, 2349.

(18) Gasperin, M.; Le Bihan, M. T. *J. Solid State Chem.* **1982**, *43* (3), 346.

(19) (a) Sanz-Garcia, J. A.; Diegue, E.; Zaldo, C. *Phys. Status Solidi A* **1988**, *108* (2), K145.

(20) (a) Domen, K.; Kudo, A.; Shibata, M.; Tanaka, A.; Maruya, K.; Onishi, T. *Chem. Soc. Chem. Commun.* **1986**, 1706. (b) Kudo, A.; Tanaka, A.; Domen, K.; Maruya, K.; Aika, K.; Onishi, T. *J. Catalysis* **1988**, *111*, 67. (c) Kudo, A.; Tanaka, K. S.; Asakura, K.; Domen, K.; Maruya, K.; Onishi, T. *J. Catalysis* **1989**, *120*, 337. (d) Sayama, K.; Tanaka, A.; Domen, K.; Maruya, K.; Onishi, T. *Catal. Lett.* **1990**, *4*, 217. (e) Sayama, K.; Tanaka, A.; Domen, K.; Maruya, K.; Onishi, T. *J. Phys. Chem.* **1990**, *95*, 1345. (f) Tanaka, A.; Kondo, J. N.; Domen, K. *Crit. Rev. Surf. Chem.* **1995**, *5*(*4*), 305.

(21) Abe, R.; Hara, M.; Kondo, J.; Domen, K. *Chem. Mater.* **1998**, *10*, 1647.

(22) Keller, S. W.; Kim, H.-N.; Mallouk, T. E. *J. Am. Chem. Soc.* **1994**, *116*, 8817.

(23) (a) Kim, Y. I.; Salim, S.; Hug, M. J.; Mallouk, T. E. *J. Am. Chem. Soc.* **1991**, *113*, 9561. (b) Kim, Y. I.; Atherton, S. J.; Brigham, E. S.; Mallouk, T. E. *J. Phys. Chem.* **1993**, *97*, 11802. (c) Saupe, G. B.; Mallouk, T. E.; Kim, W.; Schmehl, R. H.; *J. Phys. Chem.* **1997**, *101*, 2508.

(24) (a) Wadsley, A. D. *Acta Crystallogr.* **1964**, *17*, 623. (b) Andersson, S.; Wadsley, A. D. *Acta Crystallogr.* **1961**, *14*, 1245. (c) Hervieu, M.; Raveau, B. *J. Solid. State. Chem.* **1980**, *32*, 161. (d) Gasperin, P. M. *Acta Crystallogr.* **1982**, *B38*, 2024. (e) Berry, K. L.; Aftandilian, V. D.; Gilbert, W. W.; Meibohn, E. P. H.; Young, H. S. *J. Inorg. Nucl. Chem.* **1960**, *14*, 231.

(25) Olivier, J. P.; Conklin, W. B. Determination of Pore Size Distribution from Density Functional Theoretic Models of Adsorption and Condensation within Porous Solids. Presented at the International Symposium on the Effects of Surface Heterogeneity in Adsorption and Catalyst on Solids; Kazimier Dolney, Poland, July, 1992.

stantial excess of that needed to precipitate the colloid. Excess 1 M HCl was used to prepare acid-precipitated colloids. For the microtomed samples, the colloid was dispersed in acetone, HCl was added, and the precipitate was centrifuged. The supernatant was discarded and more acetone was added. After repeating this procedure four times, the acetone was removed and the sample was air-dried at 22 °C.

Transmission Electron Microscopy (TEM) and Sample Preparation. TEM images were obtained with a JEOL 1200EXII microscope using 80 kV acceleration voltage and 80 μA filament current. Samples for microtoming were prepared using Spurr's Kit from Electron Microscopy Sciences. The sample was embedded by suspending the dried tubules in a 1:1 mixture of the embedding medium and acetone. After mixing well, the mixture was allowed to stand for 30−120 min. The supernatant was decanted; a 1:3 acetone/resin mixture was added, mixed, allowed to stand, and decanted. Finally, the pure resin was added, mixed, and allowed to cure overnight at 60 °C. Microtoming of the hardened resin into thin sheets was then done to obtain cross sections of the tubules for imaging by TEM. These were lightly pressed onto carbon-coated Formvar-coated copper grids (200 mesh) for viewing. Other samples were deposited from solution by slowly applying a small drop to one side of the grid with a pipet, waiting 2 s, and then slowly drawing off the drop with the pipet.

Atomic Force Microscopy (AFM) Sample Preparation. Glass and silicon substrates were primed with 4-(aminobutyl)-dimethylmethoxysilane (United Chemical Technologies, Inc.) as previously described[26] in order to produce a positively charged surface. Coverage was monitored by ellipsometry, using a Gaertner model L2W26D ellipsometer with HeNe laser (6328 Å) light. For sample deposition, the primed substrates were immersed in the particle suspensions for 5 min followed by rinsing with water. Deposition with concurrent sonication was the same except that the suspensions were held in a conventional laboratory sonicator (Branson model 2200) during the deposition period, which was 1 min. Colloidal suspensions were subjected to turbulent flow by first forcefully squirting and sucking the colloid in and out of a bulbed pipet and into a Petri dish, and this was followed immediately by holding a primed substrate in the solution for 1 min. Alternatively, glass and silicon substrates were used without any priming monolayer, but were cleaned in a sonicated piranha solution (3:1 v/v concentrated H_2SO_4 and 30% H_2O_2). (CAUTION! Reacts violently with organic compounds.) for 10 min, rinsed with water and dried with a stream of Ar prior to use. A drop of a dilute suspension (at ~1 mg/mL) was allowed to dry on these substrates before imaging. AFM was performed with a Nanoscope IIIA system. The AFM tips and the cantilevers were made from microfabricated silicon nitride. All AFM images were collected in tapping mode. All water used in these experiments was filtered through a Barnstead Nanopure II water system.

Preparation and Immobilization of Bilayer Colloid Samples. Borosilicate glass microscope slides were sonicated in a detergent and water solution for 5 min, rinsed with water, and then sonicated in 6 M NaOH for 2 min and rinsed with water. The cleaned slides were then sonicated in 1 M $AlCl_3$ for 5 min and rinsed with water prior to immersion into the suspension of exfoliated colloid. To prepare a colloid consisting primarily of bilayers, 140 μL of TBA^+OH^- in water (Aldrich, 40% w/w) was added quickly to a stirred solution containing 0.1 g of $K_{0.8}H_{3.2}Nb_6O_{17}$ and 8 mL of water at 0 °C. The glass substrates were dipped into this suspension for 5 s, within 15 min of the addition of TBA^+OH^-. The samples were not rinsed, but excess drops of the suspension were removed by wicking them off with a tissue.

Preparation of Added Salt Solutions. Eight 11.0 mL colloidal suspensions at 0.45 mg/mL and pH 9 were prepared. The pH was adjusted with 0.1 M HCl. These suspensions were made with TBA^+Br^- added, making each of them 0.116, 0.231, 0.347, 0.928, 1.97, 2.09, 2.20, and 2.79 mM, respectively. After mixing, each suspension was allowed to stand for 10 min before obtaining TEM samples. Care was taken to use a consistent sampling technique with all samples.

Results and Discussion

The needlelike shape of the particles seen in TEM images (Figure 1a) represents individual tubules formed by the rolling up of sheets of exfoliated $K_{4-x}H_xNb_6O_{17}$ ($x \approx 3.2$). The tubules are 0.1−1 μm in length, and most have outer diameters ranging from 15 to 30 nm. Both the colloids and the precipitated tubules are stable for months or longer. Closer examination by TEM (Figure 1b) reveals similarities to images of multiwall carbon[6a] and metal disulfide[27] nanotubes, such as higher contrast regions along the sides of the tubes, where the electron beam must travel through more material. Figure 1c shows an image obtained from a more dilute colloid, which contains sheets that are partially rolled at the edges, with a flat unrolled central region. The inner part of a tubule often has more turns than the ends, because the sheets are irregular in shape. This effect is especially apparent in Figure 1c. The thinner walled ends occasionally seem wider than the middles and have an evenly gray appearance in the TEM. These observations are consistent with a slight flattening of the thinner ends of the tubules.

Similar images (resembling in particular Figure 1b) have been interpreted by Domen and co-workers as edge-on views of stacked bilayers of sheets and wide interlamellar spaces. We consider this interpretation unlikely, because it requires the lamellar solid to cleave into strips, in the direction perpendicular to the natural cleavage direction of the bulk solid. To prove this point, TEM images of microtomed, resin-embedded K^+-precipitated samples were obtained and are shown in Figure 2. In this micrograph, many of the tubules are imaged end-on, and it is clear that they have roughly elliptical open ends. The diameters of the rings (~25 nm) correspond to the diameters of the tubes inferred from side views in other TEM images (Figure 1). The wall thicknesses found in the cross-sectional views range from 2.4 to 6 nm, which corresponds to the thickness of the high contrast region observed side-on. Some tubules appear to have few turns, because no dark edge is visible in the TEM. Because the diameters of these thin tubes are close to those of the darker edged tubes, we suspect that their edge thickness is below the resolution limit (1−2 nm) of the TEM instrument. It is possible that these thin-walled tubes have collapsed during the drying process and are in fact flat. This geometry would also show evenly gray TEM images.

The size of the sheet that has rolled up to create a particular tubule can be estimated by measuring its length, wall thickness, and apparent diameter. X-ray powder diffraction patterns of the K^+-precipitated tubules give a broad peak centered at $2\theta = 8.4°$, which corresponds to a d spacing of 10.5 Å. Using this value as the spacing between the (radial) layers and taking the range of observed edge thicknesses (2.4−6 nm) and outer diameters (15−30 nm), we calculate lateral rolling dimensions of 140−550 nm. This is only slightly smaller

(26) Kim, H.-N.; Keller, S. W.; Mallouk, T. E.; Schmitt, J.; Decher, G. *Chem. Mater.* **1997**, *9*, 1414.

(27) Rapoport, L.; Bilik, Y.; Feldman, Y.; Homyonfer, M.; Cohen, S.; Tennne, R. *Nature* **1997**, *387*, 791.

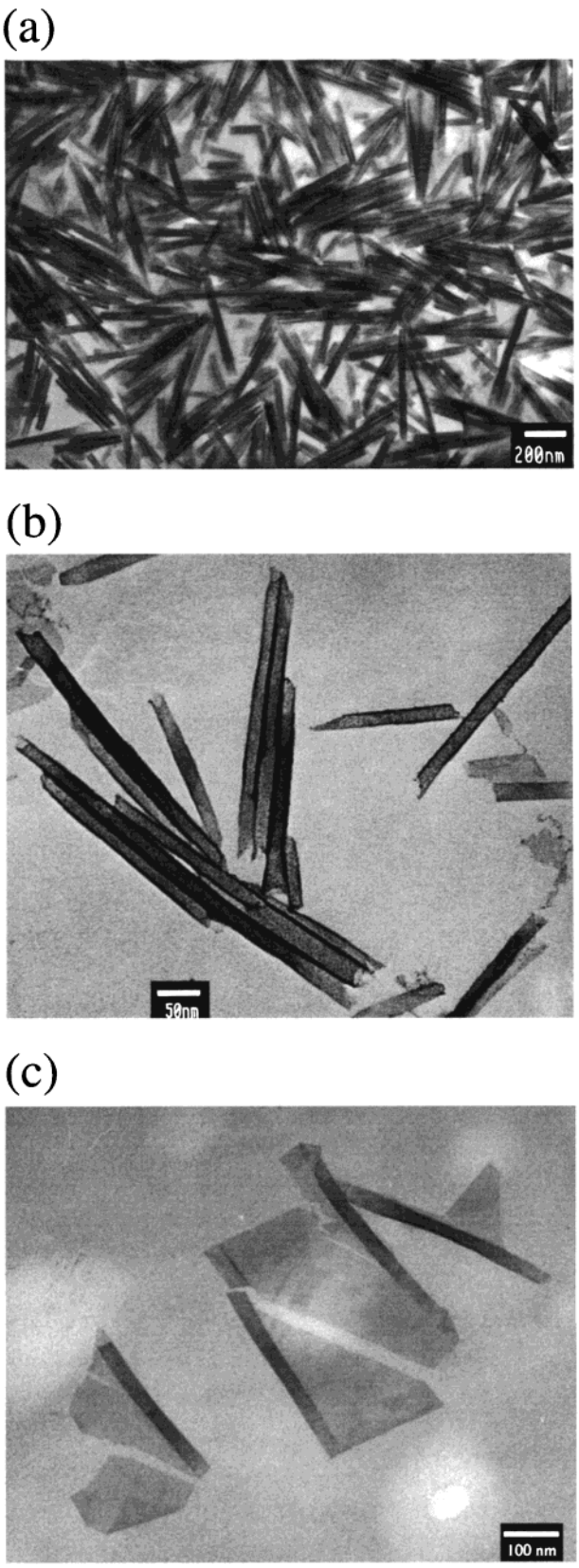

Figure 1. TEM images of exfoliated $K_{0.8}H_{3.2}Nb_6O_{17}$: (a) Sample taken from a concentrated suspension (50 mg/mL), (b) colloid precipitated with NaCl, and (c) sample taken from a dilute suspension (0.1 mg/mL).

than the dimensions of flat, uncoiled sheets derived from the same colloids (see below), and again supports the idea of tubule formation.

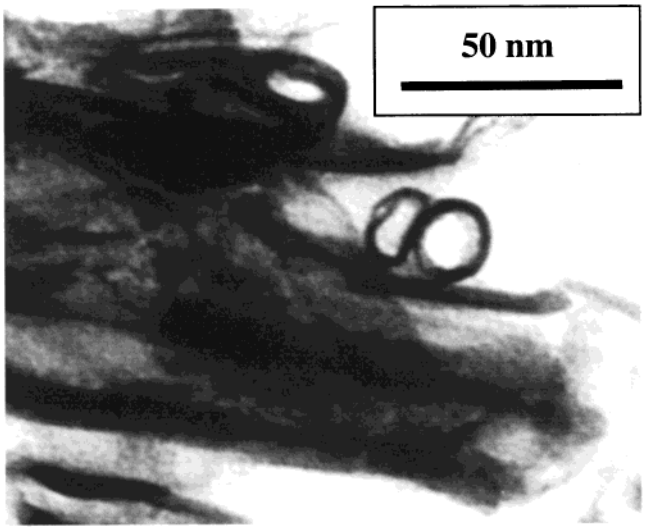

Figure 2. TEM image of precipitated colloids imbedded in a resin and microtomed to reveal a cross-sectional view of the tubules. The darker rings are the walls of tubules viewed down the long axis. HCl was used to precipitate the colloid, and the solvent was changed to acetone before drying.

Ionic strength, varied by means of added salt, and colloid dilution were investigated as possible means of controlling the coiling/uncoiling of sheets. With organic polyelectrolytes, increasing the ionic strength of the solution decreases the electrostatic repulsion of like charges, causing the polymer chain to coil.[28] Because the hexaniobate sheets (without counterions) are negatively charged, it was expected that lower ionic strength conditions would favor the uncoiling of sheets, and high ionic strength would favor the coiled form. Dilute suspensions were prepared at a concentration of 0.45 mg colloid/mL. The pH of the suspensions was 9, which implies that the concentration of free M^+OH^- (M^+ = TBA^+, K^+) is on the order of 0.01 mM. A different amount of TBA^+Br^- was added to each solution, such that the concentration varied between 0.116 and 2.79 mM. TEM images of these colloids were remarkably similar. In each image one could find roughly the same proportion of fully coiled sheets and partially unrolled or folded sheets, and from this we conclude that there is little or no effect of added TBA^+Br^- in this concentration range. Attempts to substitute alkali halide salts for TBA^+Br^- in this experiment invariably led to precipitation of aggregated tubules. On the other hand, dilution of the colloid (without added salt) has a pronounced effect on the coiling/uncoiling equilibrium. Figure 1c shows a TEM image taken from a very dilute colloid (0.1 mg/mL). This may be compared with a concentrated colloid at 50 mg/mL (Figure 1a), which shows predominantly tubules. We have also observed the uncoiling of tubules in suspensions that have been subjected to vigorous stirring, shaking, sonicating, or squirting just prior to adsorption on a cationic surface. This and the observation of mixtures of sheets and tubules in most samples suggests that there is relatively little free energy difference between the coiled and uncoiled forms of the colloid.

In the low ionic strength images and in images of uncoiled sheets deposited under conditions of flow, one

(28) Lvov, Y.; Decher, G.; Möhwald, H. *Langmuir* **1993**, *9*, 481

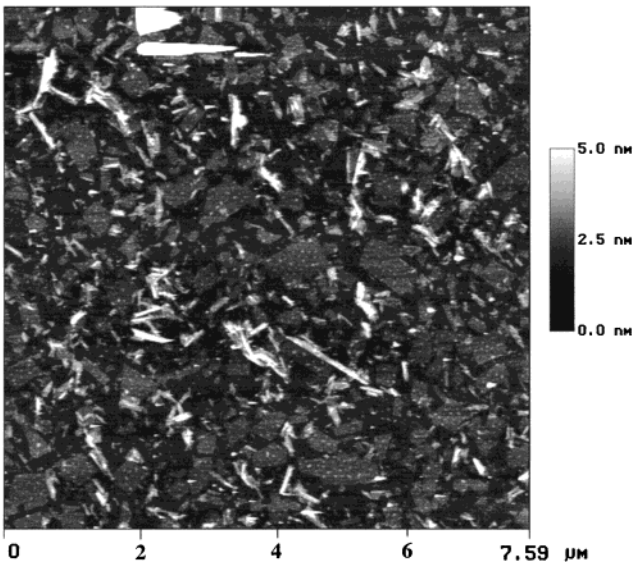

Figure 3. AFM topographic image of a colloid at pH 8.7 subjected to solution turbulence just prior to deposition onto an amine-terminated Si surface. The tubules are largely unrolled.

always observes many sheets of identical contrast in TEM images, implying that the flat regions contain exactly the same number of layers. An important question is whether these are bilayer or unilamellar particles. One might expect bilayers to be kinetically stable, since $K_4Nb_6O_{17}$ contains two chemically distinct interlayer galleries that alternate along the stacking axis, and since one of these is more rapidly exchangeable with cations than the other.[17,20] In our experiments, the ion exchange reaction with strong acid stops at a stoichiometry of about $K_{0.8}H_{3.2}Nb_6O_{17}$, where most of the K^+ ions in both interlayer galleries have been exchanged for H^+. Presumably, the remaining K^+ ions reside mainly in the slowly exchanging interlayer galleries. Interestingly, topographic measurements by AFM argue convincingly that the sheets are unilamellar; however, short exfoliation times (see below) do indeed produce bilayer colloids. Figure 3 shows an AFM image of a monolayer of unilamellar sheets adsorbed onto amine-primed Si/SiO_x under flow conditions at pH 8.7. The average height of the smooth sheets above the background is 11 Å, which is consistent with the average interlayer difference (9.4 Å) in $K_4Nb_6O_{17}\cdot 3H_2O$, and too thin to represent a bilayer film.

The precipitation of exfoliated $K_{0.8}H_{3.2}Nb_6O_{17}$ was also studied by strong acid titration. The titration curve is shown in Figure 4, plotted as pH vs TBA^+ mole fraction in $TBA_xK_{0.8}H_{3.2-x}Nb_6O_{17}$, and it is quite similar to that found with unilamellar colloids of α-zirconium phosphate and $HTiNbO_5$.[29,30] In this titration there are two equivalence points, one centered at pH 8.2, which corresponds to the formation of a single phase colloid, and a second weaker inflection point at pH 10.4, which may signal the formation of a more densely packed TBA^+ monolayer on the colloid surface. Below pH 7 the colloid begins to aggregate, and a solid precipitate is formed. Because of the existence of tubules in the

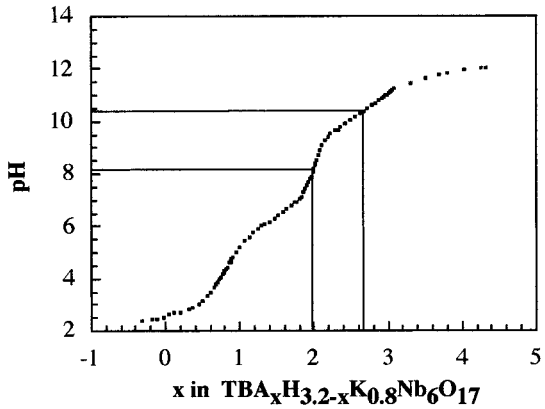

Figure 4. Titration of exfoliated $K_{0.8}H_{3.2}Nb_6O_{17}$ (12.5 mg/mL) with 34 mM HCl. Excess TBA^+OH^- was added at the beginning of the titration. The equivalence point at pH 8.2 indicates a single phase colloid.

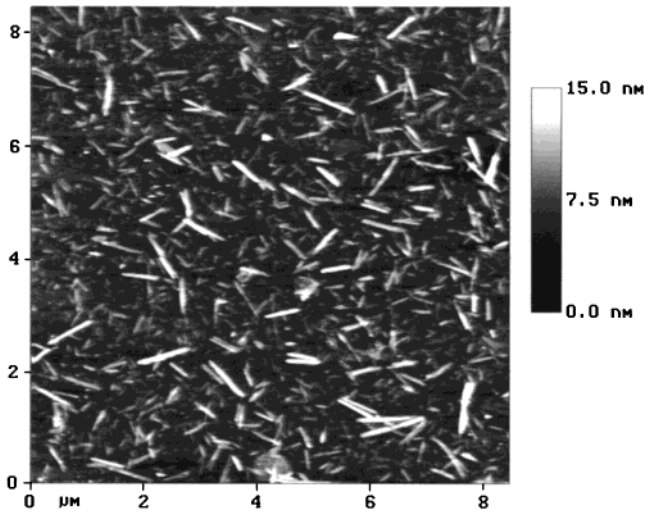

Figure 5. AFM image of exfoliated $K_{0.8}H_{3.2}Nb_6O_{17}$ deposited on an amine-functionalized Si substrate, showing that the colloid consists primarily of tubules at pH 7, regardless of solution flow conditions.

colloid, the term "restacking" is not quite appropriate, but the phenomenon is similar in the sense that the colloid is neutralized and therefore aggregates. H^+ is small enough to charge-compensate all the ion exchange sites on the basal plane surfaces, and so it displaces TBA^+ essentially quantitatively in the titration. The same is true for other small cations which cause precipitation, such as Na^+ and K^+.

In light of the observation of an equivalence point at pH 8.2, a colloidal sample was acidified to pH 7 under turbulent conditions and was then adsorbed onto amine-primed Si/SiO_x. It is evident from Figure 5 that only tubules exist at this pH, despite the conditions of flow that uncoil the colloid at higher pH. We can conclude from these observations that colloid concentration and pH exert a stronger influence on the coiling/uncoiling equilibrium than do conditions of flow. Taken together, these observations support the model sketched in Scheme 1. Acid exchange of $K_4Nb_6O_{17}$ replaces most of the K^+ ions with H^+. Exfoliation produces a bilayer colloid initially, but it transforms (depending on conditions) irreversibly into tubules, unilamellar sheets, or a mixture of both. At very low colloid concentration, K^+ and TBA^+ ions dissociate from these sheets, and the ex-

(29) Kaschak, D. M.; Johnson, S. A.; Hooks, D. E.; Kim, H.-N.; Ward, M. D.; Mallouk, T. E. *J. Am. Chem. Soc.* **1998**, *120*, 10887.
(30) Fang, M.; Kim, H.-N.; Saupe, G. B.; Miwa, T.; Fujishima, A.; Mallouk, T. E. *Chem. Mater.* **1999**, *11*, 1526.

Scheme 1. Progressive Transformation of $K_{0.8}H_{3.2}Nb_6O_{17}$ to Bilayer Sheets, Single-Sheet Tubules, and Unrolled Single-Sheet Colloids[a]

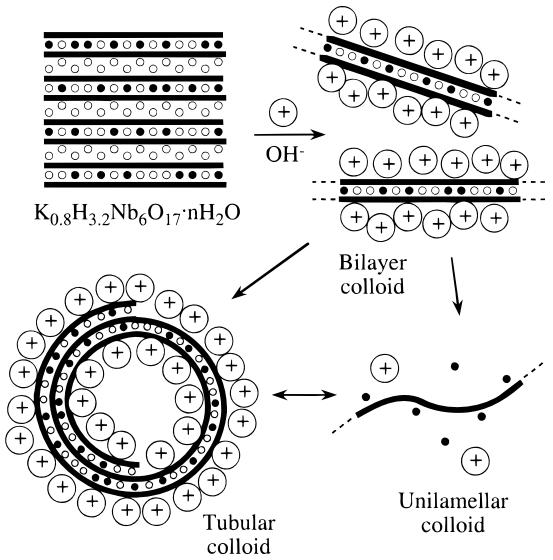

[a] Dark lines represent the niobium oxide sheets, filled circles represent K^+ ions, and open circles represent H^+ ions. The transformation from bilayer to single-sheet forms is apparently irreversible.

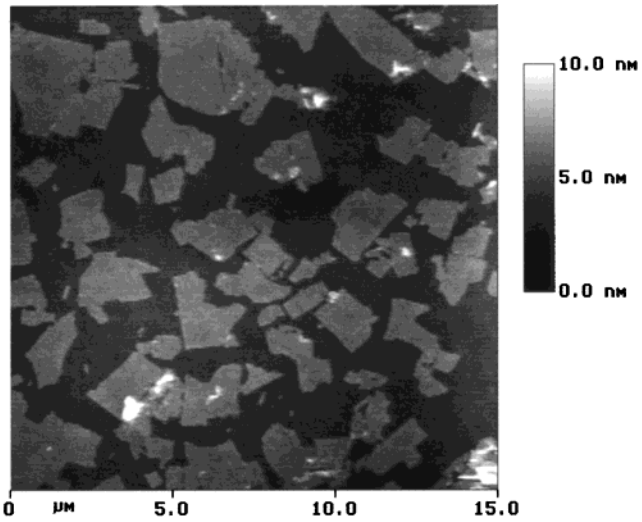

Figure 6. AFM image of bilayer sheets on a glass substrate, captured 15−20 s after the beginning of the exfoliation reaction of $K_{0.8}H_{3.2}Nb_6O_{17}$ with TBA^+OH^-. The sheets range in height from 15 to 21 Å.

tended conformation is stabilized by electrostatic repulsion. The tubular conformation allows the anionic surfaces of the sheets to aggregate around K^+ and H^+ ions, as in the bilayer colloid, but it does not require pairs of "unconnected" sheets to associate. Hence the irreversible transformation to a unilamellar (tubular or uncoiled) phase may be thought of as entropy-driven.

The sequence of steps sketched in Scheme 1 also suggests that exfoliation should produce bilayer colloids, at least in the initial stages of the reaction. Proton exchange of $K_4Nb_6O_{17}$ occurs most rapidly in alternate interlayer galleries, and subsequent treatment with TBA^+OH^- should produce colloids that consist of two sheets, sandwiching a layer of K^+ and H^+ ions. Figure 6 shows an AFM image of a sample isolated 15−20 s after addition of TBA^+OH^- to the proton-exchanged solid. The image shows flat sheets that have heights averaging 18 Å above the background. This is too thick for single sheets, but is almost exactly the thickness expected (18.8 Å) for bilayers. The height and flatness of these sheets provide good evidence that the exfoliation reaction produces bilayers initially. It should be noted that at 15 s, most of the sample is still in the form of unexfoliated crystallites. At later times, mixtures of bilayer sheets and tubules are observed.

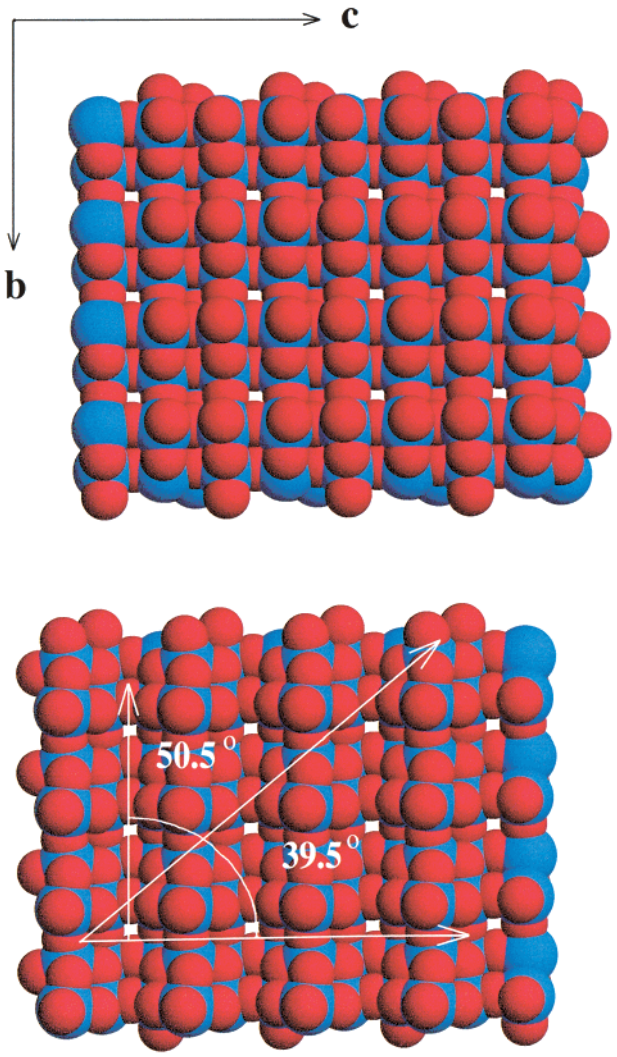

Figure 7. Space-filling model of a single hexaniobate sheet as seen from both sides. The cations are omitted for clarity. Note that one side (a) is less sterically crowded than the other.

While the model illustrated in Scheme 1 helps to explain the formation of unilamellar colloids, it does not explain why sheets derived from this particular compound, and not others with similar composition, curl to form tubules. One distinguishing feature of this compound is that individual $(-Nb_6O_{17}-)_n$ sheets do not have inversion symmetry. By way of analogy, it is interesting to note that organic tubules are also frequently derived from amphiphiles,[31−34] carbohydrates,[5c] and dendrimers[35] that lack inversion symmetry. Figure 7 shows a space-filling model of a single $Nb_6O_{17}^{4-}$ sheet

(31) Zhong-Can, O.; Jixing, L. *Phys. Rev. A* **1991**, *43*, 6826.
(32) Ratna, B. R.; Baral-Tosh, S.; Kahn, B.; Schnur, J. M.; Rudolph, A. S. *Chem. Phys. Lipids* **1992**, *63*, 47.

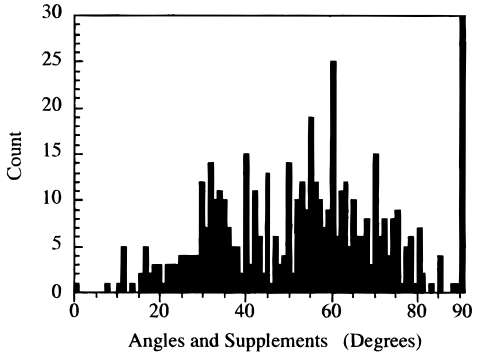

Figure 8. A histogram from the measurement of ~550 angles on single sheets. These angles are measured betweeen a sheet's straight edges; either torn, folded, or rolled.

viewed from the "heads" and "tails" sides to show both surfaces. It is clear from this figure that the top and the bottom of the sheets are different, even in the absence of counterions. One side of the sheet is more sterically crowded than the other, and once the sheets are freed of their face-to-face interaction in the solid, they may relieve strain by bending away from the crowded side. Note that this model also explains the lack of curvature seen in (face-to-face) bilayer colloids, which are found at the beginning of the exfoliation reaction.

Without knowledge of the specific interactions between the cations and the sheets, we cannot be sure that this is the preferred coiling direction. Likewise, we do not yet have an experimental means of determining whether the sheets always curl to the same side. If they do, it might be interesting to attempt to orient them in composites for the purpose of examining their nonlinear optical properties.

Crystals of $K_4Nb_6O_{17}$ cleave predominantly between the layers perpendicular to the stacking axis.[36] In TEM images of the colloids, the single sheets show signs of breaking, folding and rolling along specific in-plane crystal directions. With partially curled sheets, it is often possible to measure the angle between a sheet's edge and the long axis of the nascent tubule. To investigate the possibility that the curling direction is correlated with specific crystal planes, we measured about 550 such angles from TEM images. Care was taken to select sheets that were free of interferences of neighboring sheets, to ensure that the two edges forming the angle belonged to the same sheet. Figure 8 shows the histogram of angles derived from these measurements. For angles greater than 90°, supplementary angles are plotted. The histogram shows complementary broad maxima at angles of 35 and 55°. There is a reasonable match between these peak values and the directions of low index planes that intersect the sheets. For example, the 011 planes intersect the *y*- and *z*-axes at angles of 39.5 and 50.5°. In Figure 7b, lines

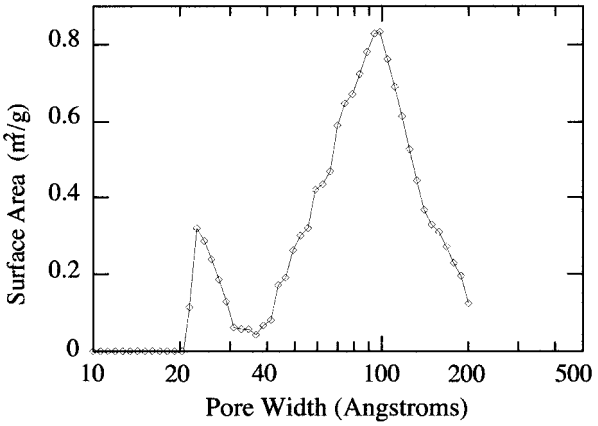

Figure 9. Pore size distribution of an acid-precipitated hexaniobate colloid.

are drawn on the sheet to illustrate the angles between these crystal planes.

BET surface area analysis of the dried tubular colloid gives a total surface area of 37 m^2/g and shows a peak in the pore size distribution at 10 nm (Figure 9). This is in good agreement with the inner diameter measured by TEM. Domen and co-workers also found that the pore diameter of acid-washed colloids, which were precipitated in the presence of MgO particles, peaked in the 10−15 nm range. By contrast, the surface area of a $HTiNbO_5$ colloid, exfoliated and restacked under identical conditions, was 5.8 m^2/g, and the major pore diameter peak was 2 nm. Again, the contrast is striking, and the pore diameter in particular is diagnostic of the difference between lamellar and tubular colloids.

Conclusions

Acid-exchanged potassium hexaniobate appears from TEM, AFM, and pore size measurements to form a tubular colloid when exfoliated with TBA^+OH^-. In the presence of excess acid, about 80% of the potassium ions in $K_4Nb_6O_{17}$ are replaced by protons. The remaining potassium ions ions are presumed to reside primarily in the more slowly exchanging of the two in interlayer galleries that alternate along the stacking axis. The bilamellar colloid that is initially formed by reacting this material with TBA^+OH^- is unstable with respect to formation of unilamellar sheets and tubules. Both the concentration of colloid and the pH are important in controlling the coiling/uncoiling equilibrium, and both H^+ and alkali ions are effective in precipitating aggregated tubules. We believe that the earlier study of Domen and co-workers on the same chemical system can be reinterpreted in terms of tubules. It is interesting that this open form of the lamellar material is more active as water photolysis catalysts than the parent solid.[15] This suggests that these tubules may be useful building blocks for artificial photosynthetic assemblies.

Acknowledgment. We thank Stacy Johnson for conducting the BET analysis, and Sherman Ponder for performing elemental analyses. This work was supported by the Division of Chemical Sciences, Office of Basic Energy Sciences, Department of Energy, under contract DE-FG02-93ER14374.

CM981136N

(33) Singh, A.; Burke, T. G.; Calvert, J. M.; Georger, J. H.; Herendeen, B.; Price, R. R.; Schoen, P. E.; Yager, P. *Chem. Phys. Lipids* **1998**, *47*, 135.

(34) Singh, A.; Schoen, P. E.; Schnur, J. M. *J. Chem. Soc., Chem. Commun.* **1988**, 1222−1223.

(35) Hudson, S. D.; Jung, H.-T.; Percec, V.; Cho, W.-D.; Johansson, G.; Ungar, G.; Balagurusamy, V. S. K. *Science* **1997**, *278*, 449.

(36) The crystal structure of $K_4Nb_6O_{17}$ was solved by Gasperin and Le Bihan[18] in space group $P2_1nb$, which is a nonstandard setting of $Pna2_1$. In either case the stacking axis is perpendicular to the *n*-glide plane, which passes through the midpoint of interlayer gallery II.